Available online at www.sciencedirect.com
ScienceDirect
Nuclear Physics B Proceedings Supplement 00 (2014) 1–6
Nuclear Physics B Proceedings Supplement

Comparison of test beam data from imaging calorimeters with Geant4 simulations

Eva Sicking on behalf of the CALICE collaboration
CERN, 1211 Geneva 23, Switzerland

Abstract

The highly granular calorimeter prototypes of the CALICE collaboration have provided large data samples with precise three-dimensional information on hadronic showers with steel and tungsten absorbers and silicon, scintillator and gas detector readout. From these data sets, detailed measurements of the spatial structure, including longitudinal and radial shower profiles and of the shower substructure are extracted. Dedicated experiments with scintillator and RPC active elements extend these measurements to include information on the time structure of hadronic showers. These results are confronted with Geant4 simulations with different hadronic physics models, presenting new challenges to the simulation codes and providing the possibility to validate and improve the simulation of hadronic interactions in high-energy physics detectors.

Keywords: CALICE, high-granularity calorimeter, Geant4

1. Introduction

The CALICE collaboration has constructed prototypes of imaging electromagnetic calorimeters (ECAL) and hadronic calorimeters (HCAL) using steel (Fe) and tungsten (W) as absorber material. Silicon (Si) and scintillator (Sc) are used for analogue readout (A) and resistive plate chambers for digital (D, one threshold) or semi-digital (SD, 3 thresholds) readout.
With 30 to 38 alternating absorber-sensor layers per prototype, the ECAL prototypes have a volume of approximately $0.2 \times 0.2 \times 0.3\,\mathrm{m}^3$, the HCAL prototypes of approximately $1 \times 1 \times 1\,\mathrm{m}^3$. The readout cell sizes range from $0.5 \times 4.5\,\mathrm{cm}^2$ to $1 \times 1\,\mathrm{cm}^2$ in the ECALs and from $3 \times 3\,\mathrm{cm}^2$ to $1 \times 1\,\mathrm{cm}^2$ in the HCALs resulting in 2,000 to 500,000 readout channels per prototype.
The detector concepts have been tested and characterised in 2006–2012 in test beam experiments at CERN and Fermilab using beams of charged leptons and hadrons with beam momenta from 1 to 300 GeV. The results of experiments with beam momenta up to 100 GeV are compared to Geant4 simulations [1, 2] using selected Geant4 physics lists recommended for the studied use cases. Over the extended time span of the presented studies, Geant4 developments have been followed by using latest Geant4 versions resulting in comparisons to versions from 9.3.p03 to 9.6.p01.

2. Validation of detector simulation

Electromagnetic processes are well understood. Comparisons between data from test beam experiments and Monte Carlo (MC) simulations of electromagnetic processes allow, on the one hand, for a cross check of the detector calibration, and on the other hand, they can give insight into requirements for details needed in detector simulations.
The calorimeter response in terms of measured visible energy $\langle E_{\mathrm{vis}} \rangle$ to $e^{\pm}$ induced showers at beam momenta of 1–50 GeV of the CALICE prototypes Si-W-ECAL, with a depth of 24 radiation lengths (X_0) [4],

Email address: eva.sicking@cern.ch (Eva Sicking on behalf of the CALICE collaboration)

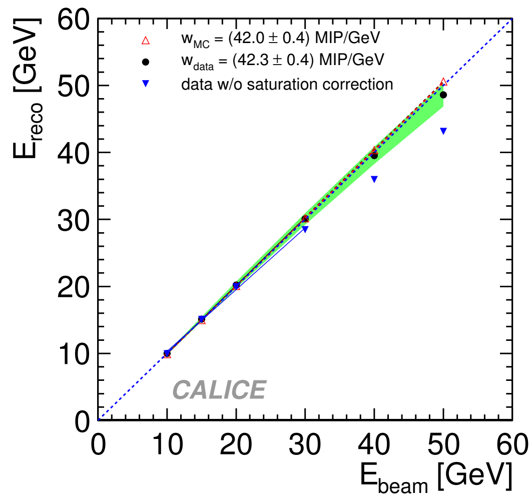

Figure 1: The mean visible positron energy as a function of the beam momentum measured with the CALICE Sc-Fe-AHCAL in comparison to simulations of Geant4 version 9.4.p02 [3].

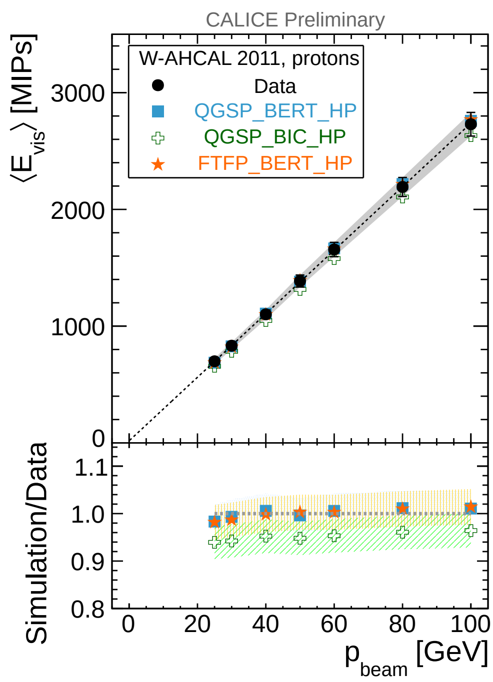

Figure 2: The mean visible proton energy as a function of the beam momentum measured at the CALICE Sc-W-AHCAL in comparison to simulations of Geant4 version 9.5.p01 [7].

Sc-W-ECAL (21 X_0) [5], Sc-Fe-AHCAL (47 X_0) [3], and Sc-W-AHCAL (85–108 X_0) [6, 7] increases linearly as a function of the beam momentum. The response of data and simulation of all prototypes agrees at the 5% level within the systematic uncertainties, with the tendency of a better agreement at low beam momenta, as shown in figure 1 as an example for 10–50 GeV positrons measured with the Sc-Fe-AHCAL. Here, the error bars indicate the statistical uncertainty and the bands the systematic uncertainties.
The energy resolutions $\sigma_{E_{\mathrm{vis}}}/E_{\mathrm{vis}}$ of the calorimeters is parametrised with the function

$$\frac{\sigma_{E_{\mathrm{vis}}}}{E_{\mathrm{vis}}} = \frac{a}{\sqrt{E[\mathrm{GeV}]}} \oplus b \oplus \frac{c}{E[\mathrm{GeV}]}, \qquad (1)$$

where a is the stochastic term, b is the constant term, and c is the noise term. The stochastic term for $e^{\pm}$ showers ranges from approximately 13% $\sqrt{\mathrm{GeV}}$ estimated for the Sc-W-ECAL at 2–32 GeV to approximately 30% $\sqrt{\mathrm{GeV}}$ estimated for the Sc-W-AHCAL at 1–6 GeV in data and simulation. b is in the order of 1% and c is determined by the electronics noise in the considered fiducial volume with values up to 60 MeV.
In addition, electromagnetic shower shapes such as the longitudinal or radial shower development are studied. For all observables, data and simulation agree within the systematic uncertainties at the 1–5% level.

3. Geant4 comparison to hadron data

The physics of hadronic showers including current knowledge of hadronic nuclear interactions is modelled in MC simulations. A data-MC comparison of hadronic interactions can challenge these models based on the studied observables. Here, the CALICE test beam experiments give a unique opportunity to study high-resolution shower shapes, the shower sub-structure and the shower time structure.

3.1. Calorimeter response

The calorimeter response in terms of the visible energy $\langle E_{\mathrm{vis}} \rangle$ to hadron beams as a function of the beam momentum is studied and compared to Geant4 simulations for $\pi^{\pm}$ at 8–80 GeV for the Si-W-ECAL, with a depth of 1 interaction length (λ_{I}) [8], for $\pi^{\pm}$ at 8–100 GeV for the Sc-Fe-AHCAL (5.3 λ_{I}) [9, 10] and for π^{+} at 3–100 GeV, p at 4–100 GeV, and K^{+} at 50 GeV and 60 GeV for the Sc-W-AHCAL (3.9–4.9 λ_{I}) [6, 7]. As an example, the Sc-W-AHCAL response for protons at 25–100 GeV is shown in figure 2 in comparison to Geant4 simulations. The response of the detector increases linearly as a function of the beam momentum for both data and the Geant4 models. Data and Geant4 agree within the systematic uncertainties of 5% for all studied physics lists.

QGSP_BERT_HP and FTFP_BERT_HP achieve a better agreement of within 1%. In general, the calorimeter response of all prototypes compared to the recommended Geant4 models agree to better than 10%.

3.2. Energy resolution

The hadron energy resolution $\sigma_{E_{\rm vis}}/E_{\rm vis}$ is estimated for $\pi^{\pm}$ at 8–100 GeV for the Sc-Fe-AHCAL [9, 11] and for π^{+} at 3–100 GeV and p at 4–100 GeV for the Sc-W-AHCAL [6, 7]. As for the electromagnetic showers, the energy resolution can be parametrised with equation 1. To compare the different readout modes, the energy resolution for π^{-} at 10–80 GeV for the Sc-Fe-AHCAL is shown in the top panel of figure 3 for analogue, digital, and semi-digital readout [11]. For the digital and the semi-digital readout options tested for the Sc-Fe-AHCAL with a cell size of $3 \times 3\,\text{cm}^2$, the energy resolution fit was complemented with a term for saturation and leakage effects. In addition to the analogue Sc-Fe-AHCAL resolution, a combined analogue resolution of the Sc-Fe-AHCAL and the tail catcher-muon tracker (TCMT, 5.8 $\lambda_{\rm I}$), which recovers shower energy from longitudinal leakage, is shown as well as the combined Sc-Fe-AHCAL+TCMT resolution estimated using software compensation techniques [9]. The stochastic term of the analogue energy resolution fit for the CALICE prototypes ranges from 45% $\sqrt{\text{GeV}}$ estimated for the Sc-Fe-AHCAL in combination with the TCMT and software compensation for $\pi^{\pm}$ at 10–80 GeV to approximately 62% $\sqrt{\text{GeV}}$ for $\pi^{\pm}$ 3–10 GeV and 63% $\sqrt{\text{GeV}}$ for p at 4–10 GeV in the Sc-W-AHCAL. The constant term b has values of 1–11% and the noise term c is determined by the electronics noise in the full calorimeter stack with values up to 200 MeV. The energy resolution estimated in Geant4 simulations is mostly slightly better than for data, as visible in the bottom panel of figure 3.

3.3. Shower shapes

The high granularity of the CALICE prototypes allows for a study of shower shapes with unprecedented resolution. The longitudinal and radial shower development are studied for $\pi^{\pm}$ at 2–80 GeV in Si-W-ECAL [8, 12], for $\pi^{\pm}$ and p at 8–100 GeV for the Sc-Fe-AHCAL [9, 10] and for π^{+} at 3–100 GeV and p at 4–100 GeV for the Sc-W-AHCAL [6, 7]. As an example for longitudinal shower shapes, the mean of the longitudinal energy profile is shown in figure 4 for π^{-} at 2–10 GeV in the Si-W-ECAL in comparison to Geant4 simulations. In comparison to data, the models deposit more energy near the interaction layer resulting in a lower mean value

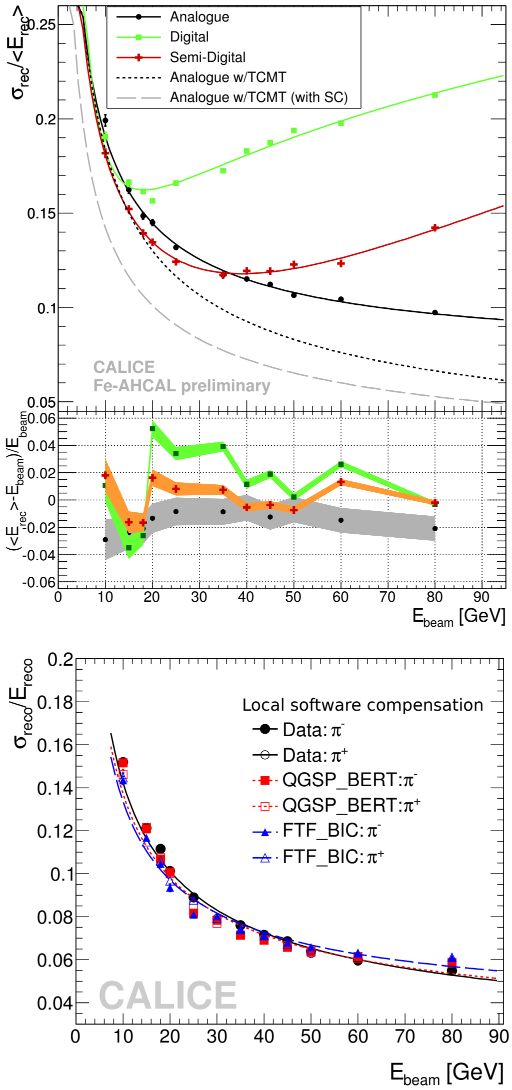

Figure 3: Top panel: Pion energy resolution as a function of the beam momentum measured with the CALICE Sc-Fe-AHCAL obtained using different approaches of the energy reconstruction: analogue, digital, and semi-digital[11].
Bottom panel: Pion energy resolution as a function of the beam momentum measured with the CALICE Sc-Fe-AHCAL+TCMT after applying software compensation in comparison to simulations of Geant4 version 9.4 [9]. See text for explanations.

of the longitudinal energy profile. The effect increases with beam momentum. The best description of this observable for Si-W-ECAL pion data is given by the QGSP_BERT physics list with an overall agreement at the 4% level.

To extract additional information, the longitudinal and radial energy profiles are parametrised [13]. For ex-

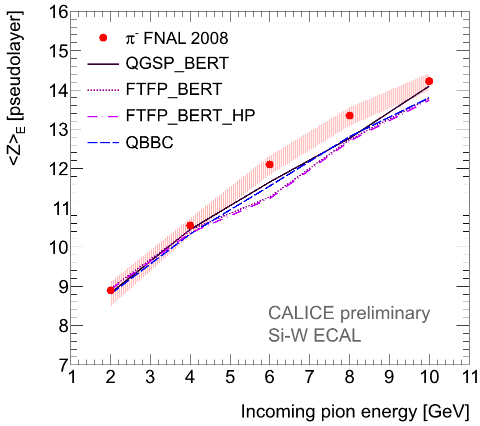

Figure 4: Mean of the longitudinal energy profile for interacting hadron events as a function of beam energy measured with the CALICE Si-W-ECAL in comparison to simulations of Geant4 version 9.6.p01 [12].

ample, the longitudinal energy profiles as shown in the top panel of figure 5 for 40 GeV π^+ measured with the Sc-Fe-AHCAL are described with the sum of two gamma distributions

$$\Delta E = A \cdot \left\{ \frac{f \cdot \exp(-\frac{z}{\beta_{\rm short}})}{\beta_{\rm short} \cdot \Gamma(\alpha_{\rm short})} \cdot \left(\frac{z}{\beta_{\rm short}}\right)^{\alpha_{\rm short-1}} + \frac{(1-f) \cdot \exp(-\frac{z}{\beta_{\rm long}})}{\beta_{\rm long} \cdot \Gamma(\alpha_{\rm long})} \cdot \left(\frac{z}{\beta_{\rm long}}\right)^{\alpha_{\rm long-1}} \right\}, \quad (2)$$

where A is a scaling factor, α and β are shape and slope parameters of the short and the long component, and f indicates the relative contribution of the short component to the overall longitudinal energy profile. As an example, the parameter f is shown for π and p induced showers at 10–80 GeV in the Sc-Fe-AHCAL in the bottom panel of figure 5 in comparison to Geant4 simulations. QGSP_BERT overestimates the short component in pion and proton showers, FTFP_BERT only overestimates the short component in pion showers but gives a good description for protons.

As an example for radial shower shapes, the mean energy-weighted shower radius as a function of the beam momentum for protons at 25–100 GeV in the Sc-W-AHCAL is shown in figure 6 in comparison to Geant4 simulations [7]. As all models overestimate the energy deposition close to the shower core (figure not shown, see [7]), they underestimate the mean energy-weighted radius. The best description for protons in the Sc-W-AHCAL for this observable is given by the FTFP_BERT_HP model.

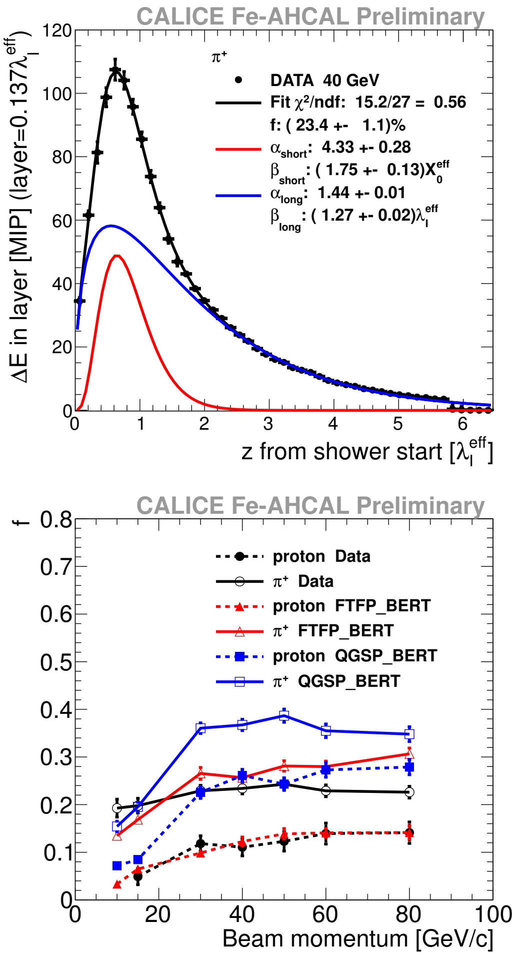

Figure 5: Top panel: Fit (black curve) of longitudinal energy profile of 40 GeV pion showers measured with the CALICE Sc-Fe-AHCAL, where the red and blue curves show the contributions of the short and long components, respectively [13]. See text for explanations.
Bottom panel: The relative contribution of the short component f to the longitudinal energy profiles as a function of the beam momentum measured with the CALICE Sc-Fe-AHCAL in comparison to results from simulations of Geant4 version 9.6.p01[13].

3.4. Shower substructure

The high granularity of the calorimeter prototypes also allows for an exploration of the substructure of hadronic showers. A good description of the shower substructure is crucial for reliable simulation studies in the detector development phase for particle flow detectors.

The substructure is studied using track segments of minimum ionising particles within hadronic showers. The analysis is performed for π^+ at 10–80 GeV in the Sc-Fe-AHCAL [15] and for π^+ at 10–80 GeV in the Fe-SDHCAL [14]. As an example, the multi-

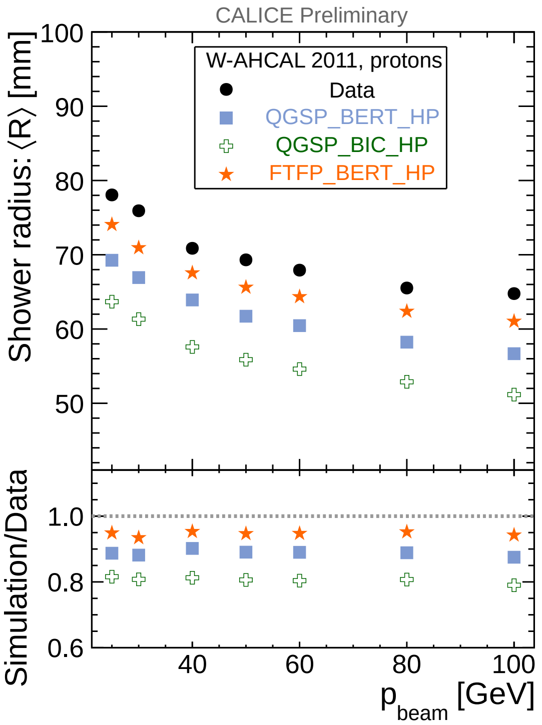

Figure 6: The mean energy-weighted shower radius as a function of the beam momentum for protons measured with the CALICE Sc-W-AHCAL in comparison to simulation results of Geant4 version 9.5.p01 [7].

plicity of identified track segments is shown for the Fe-SDHCAL in figure 7 in comparison to Geant4 simulations. QGSP_BERT_HP gives the best agreement with the Fe-SDHCAL data for this observable at the 5% level.

3.5. Shower time structure

The test beam campaigns of the W-AHCAL and the Sc-Fe-SDHCAL included the Tungsten Timing Test Beam (T3B) experiment [16]. T3B consists of an array of scintillator cells with high time resolution readout placed behind the main calorimeter stack. It allows to study the time structure of the hadronic showers by detecting the arrival time of hits from the hadron shower after traversing the calorimeter stack. Special interest lays in delayed components of the hadronic showers which are, for example, due to nuclear de-excitation and neutron propagation, assumed to play a more important role in case of tungsten absorbers than in steel absorbers. The distribution of arrival times of identified hits for pion induced showers at 60 GeV in tungsten is shown in figure 8 in comparison to Geant4 simulations. In addition, the radial profile of the mean time

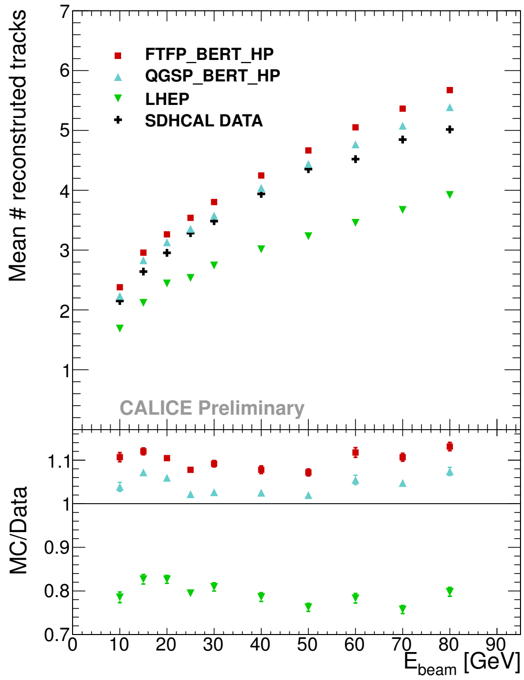

Figure 7: Mean number of reconstructed tracks in hadronic showers as a function of the beam energy measured with the CALICE Fe-SDHCAL in comparison to simulations of Geant4 version 9.6.p01 [14].

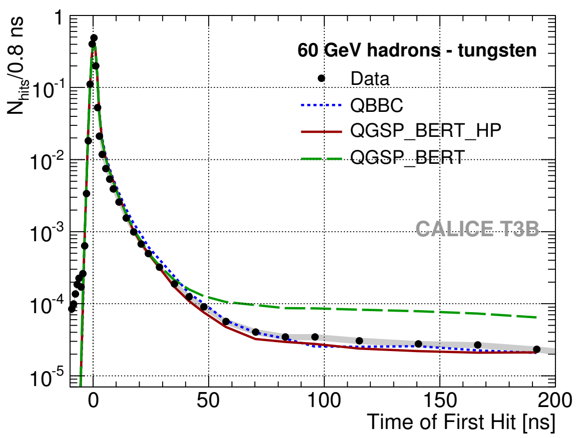

Figure 8: The distribution of the time of the identified hits in the CALICE T3B from hadron induced showers at 60 GeV in a calorimeter stack with tungsten as absorber in comparison to simulations of Geant4 version 9.3.p03 [16].

of first hit is shown in figure 9. While all studied models give a good description for steel absorbers (figures not shown, see [16]), a good agreement for the tungsten absorber is only achieved for the models QBBC

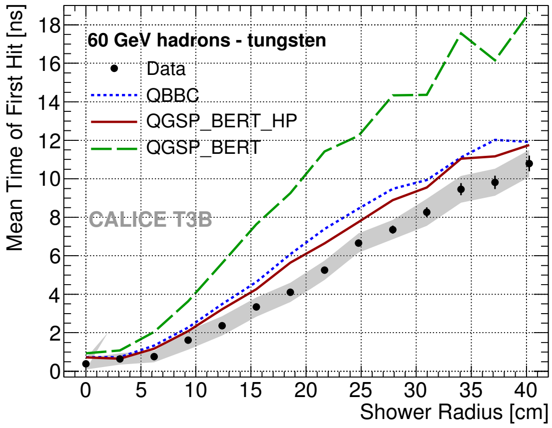

Figure 9: The radial profile of the mean time of first hit measured with the CALICE T3B for hadron induced showers at 60 GeV in a calorimeter stack with tungsten as absorber in comparison to simulations of Geant4 version 9.3.p03 [16].

and QGSP_BERT_HP, both of which contain a high precision neutron tracking (HP) package. At time of first hit values above 50 ns, relevant for the outer part of the hadron showers, the model QGSP_BERT without the HP package disagrees strongly with the tungsten data.

4. Summary and outlook

The CALICE collaboration has performed test beam experiments with highly granular ECAL and HCAL prototypes. These experiments tested for the first time novel technologies in large-scale, fine-grained calorimeters and demonstrated the capability to calibrate the vast number of readout channels. The CALICE prototypes studied the particle shower evolution with unprecedented spatial and time resolution, which challenges existing simulation codes.

Electromagnetic processes are used to validate the implementation of the detector simulation and to cross check the detector calibration. For all prototypes, a good agreement between data and detector simulation at the 1–5% level is achieved. A comparison between data and Geant4 simulation for hadron showers allowed to test the Geant4 models of hadronic nuclear interactions. The agreement between data and Geant4 simulations depends on particle, energy and physics lists. Selected Geant4 physics lists recommended for the studied use cases reproduce the hadronic data at the level of 10%. It was found that the high precision neutron tracking extension of the physics list improves tungsten HCAL simulation.

The analysis and comparison to Geant4 simulations of hadronic data using an extended beam momentum range and for calorimeter prototypes using gaseous readout are under way and will allow for a test of the latest version of Geant4 models.

References

[1] S. Agostinelli, et al., Geant4: A Simulation toolkit, Nucl. Instrum. Meth. A506 (2003) 250. doi:10.1016/S0168-9002(03)01368-8.

[2] J. Allison, et al., Geant4 developments and applications, IEEE Trans. Nucl. Sci. 53 (2006) 270. doi:10.1109/TNS.2006.869826.

[3] C. Adloff, et al., Electromagnetic response of a highly granular hadronic calorimeter, JINST 6 (2011) P04003. arXiv:1012.4343, doi:10.1088/1748-0221/6/04/P04003.

[4] C. Adloff, et al., Response of the CALICE Si-W electromagnetic calorimeter physics prototype to electrons, Nucl. Instrum. Meth. A608 (2009) 372. doi:10.1016/j.nima.2009.07.026.

[5] CALICE Collaboration, Update of the Analysis of the Test Beam Experiment of the CALICE ScECAL Physics Prototype, CALICE analysis note 16b (2012).

[6] C. Adloff, et al., Shower development of particles with momenta from 1 to 10 GeV in the CALICE Scintillator-Tungsten HCAL, JINST 9 (2014) P01004. arXiv:1311.3505, doi:10.1088/1748-0221/9/01/P01004.

[7] CALICE Collaboration, Shower development of particles with momenta from 10 to 100 GeV in the CALICE scintillator-tungsten HCAL, CALICE analysis note 44 (2013).

[8] C. Adloff, et al., Study of the interactions of pions in the CALICE silicon-tungsten calorimeter prototype, JINST 5 (2010) P05007. arXiv:1004.4996, doi:10.1088/1748-0221/5/05/P05007.

[9] C. Adloff, et al., Hadronic energy resolution of a highly granular scintillator-steel hadron calorimeter using software compensation techniques, JINST 7 (2012) P09017. arXiv:1207.4210, doi:10.1088/1748-0221/7/09/P09017.

[10] C. Adloff, et al., Validation of GEANT4 Monte Carlo Models with a Highly Granular Scintillator-Steel Hadron Calorimeter, JINST 8 (2013) 07005. arXiv:1306.3037, doi:10.1088/1748-0221/8/07/P07005.

[11] CALICE Collaboration, Analogue, digital and semi-digital energy reconstruction in the CALICE AHCAL, CALICE analysis note 49 (2014).

[12] CALICE Collaboration, Interactions of Pions in the CALICE Silicon-Tungsten Calorimeter Prototype, CALICE analysis note 50 (2014).

[13] CALICE Collaboration, Parametrisation of hadron shower profiles in the CALICE Sc-Fe AHCAL, CALICE analysis note 48 (2014).

[14] CALICE Collaboration, Tracking within Hadronic Showers in the SDHCAL prototype using Hough Transform Technique, CALICE analysis note 47 (2014).

[15] C. Adloff, et al., Track segments in hadronic showers in a highly granular scintillator-steel hadron calorimeter, JINST 8 (2013) P09001. arXiv:1305.7027, doi:10.1088/1748-0221/8/09/P09001.

[16] C. Adloff, et al., The Time Structure of Hadronic Showers in highly granular Calorimeters with Tungsten and Steel Absorbers, JINST 9 (2014) P07022. arXiv:1404.6454, doi:10.1088/1748-0221/9/07/P07022.